UNIVERSITY OF CRETE

DEPARTMENT OF PHYSICS

MSc THESIS

Search for AGN jet alignments in the Very Large Array Sky Survey data

Ioannis Orfanos

Advisor: *Dr.* Carolina Casadio - University of Crete
Dr. Dmitriy Blinov - University of Crete

UNIVERSITY OF CRETE
DEPARTMENT OF PHYSICS

MSc THESIS

Defended by
Author Ioannis Orfanos

Search for AGN jet alignments in the Very Large Array Sky Survey data

COMMITTEE

Dr.	Carolina Casadio	-	University of Crete
Prof.	Vasiliki Pavlidou	-	University of Crete
Prof.	Andreas Zezas	-	University of Crete

Date of the defense:
10/10/2023

Περίληψη

Πολυάριθμες έρευνες έχουν αναφέρει ότι το επίπεδο πόλωσης της εκπομπής Ενεργειακών Γαλαξιακών Πυρήνων και οι κύριοι άξονες των εξωγαλαξιακών ραδιοπηγών ευθυγραμμίζονται σε μεγάλες περιοχές του ουρανού. Ωστόσο, τέτοιες ευθυγραμμίσεις παραμένουν ακόμα αβέβαιες και είναι δύσκολο να δικαιολογηθεί η ύπαρξη τους στο πλαίσιο της σύγχρονης κοσμολογίας.

Σε αυτή την εργασία, παρουσιάζουμε το μεγαλύτερο δείγμα δεδομένων από πίδακες ενργών γαλαξιακών πυρήνων, κλίμακας *kiloparsec*, έως σήμερα, το οπίο προέρχεται από τα δημοσίως διαθέσιμα δεδομένα του *Very Large Array Sky Survey*. Χρησιμοποιούμε αυτά τα δεδομένα για να ερευνήσουμε την παρουσία σημαντικών ευθυγραμμίσεων σε περιοχές του βόρειου ουρανού, όπου ραδιοπίδακες από *quasar* κλίμακας *parsec* βρέθηκαν να έχουν στατιστικώς σημαντικές ευθυγραμμίσεις. Επιπρόσθετα, αναλύουμε αυτή την ομάδα δεδομένων ώστε να διερευνήσουμε για άλλες πιθανές περιοχές με σημαντικές ευθυγραμμίσεις.

Abstract

Numerous studies have reported that the polarization plane in the emission of Active Galactic Nuclei and the major axes of extragalactic radio sources align in large regions of the sky. However, such alignments remain elusive, and justifying their existence within the framework of modern cosmology is challenging.

In this study, we present the largest sample of kiloparsec-scale AGN jets to date, derived from publicly available Very Large Array Sky Survey data. We utilize these data to investigate the presence of significant alignments in the northern sky regions, where parsec-scale quasar radio jets have been found to exhibit high statistical alignments. Additionally, we analyze this dataset to search for other potential regions with significant jet alignments.

Contents

1 Introduction

The detection of cosmological structures assumes a pivotal role in our effort to understand the structure of the universe. Large-scale structures (LSS), such as filaments, are believed to have arisen due to gravitational instabilities in the early universe, driven by primordial small density perturbations (Friday (2020)). As a consequence, investigations have been performed to unveil such structures in the expanding universe. The quest for these structures entails meticulous examination of the clustering patterns of constituent objects or the discernment of shared characteristics among them (Komberg et al. (1996),Clowes et al. (2013),Lietzen et al. (2016)). Notably, the alignment of vectors of polarized light within these structures unveils the existence of extraordinarily vast-scale formations, potentially spanning gigaparsecs (Gpc) in extent. This finding poses a formidable challenge to the prevalent model of a uniform and isotropic universe (Kumar Aluri et al. (2023)Friday (2020)), emphasizing the importance of seeking aligned structures in the universe.

A promising approach to detecting the alignments mentioned above involves the study of light polarization, as intrinsic polarization correlates with an object's morphology (Blinov et al. (2020)). Specifically, QSO[1] (Quasi-stellar object) light exhibits linear polarization at the level of 1% at optical wavelengths (Hutsemekers (1998a)). This characteristic has been exploited by Hutsemekers (1998a) to reveal the aligned polarization vectors of 170 polarized QSOs at the Gpc scale, at a redshift of z=1.5. Subsequent surveys have corroborated these findings, utilizing larger samples of polarized

[1]QSO is a term typically referring to any object that shares the characteristics of quasars (a subclass of AGNs with the main characteristic of being extremely luminous objects compared to the rest of AGNs, due to a supermassive black hole in its centre that is acreeting matter), with the main difference being that they may not exhibit the high radio luminosity that quasars usually have.

QSOs and extending the search to redshifts up to 2.5 (Kumar Aluri et al. (2023)Friday (2020)). Similar investigations have been carried out at radio wavelengths, with Joshi et al. (2007) and Tiwari and Jain (2012) employing a sample of over 4000 radio sources from the JVAS/CLASS survey. While Joshi et al. (2007) found alignments only at the 150 Mpc scale, Tiwari and Jain (2012) detected alignments within the QSO sub-sample at the Gpc scale. The latter, while potentially subject to data biases, notably overlaps with the regions exhibiting alignment in optical polarized light. Additionally, Tiwari and Jain (2019) reported radio polarization alignments with scales reaching up to 800 Mpc.

Another avenue for seeking alignments involves the exploration of coherency in the distribution of galaxies' spins. Digital sky surveys have facilitated the statistical analysis of galaxies, involving both manual and algorithmic methods for spin determination. While manual methods are prone to human-based perception biases and unsuitable for large samples, algorithmic approaches can be applied to extensive datasets and, when generated by model-driven algorithms, can produce reliable results (Kumar Aluri et al. (2023)). Such intrinsic alignments of galaxies are extensively discussed in the literature (d'Assignies D. et al. (2021), Georgiou et al. (2019)). They can be a severe source of error in weak-lensing studies (Camelio and Lombardi (2015)).

To find such aligned structures we make use of the jet emission from AGNs (active galactic nuclei). AGNs contain an super massive black hole in their center with typical mass values of $10^6 M_{\odot}$. The gravitational pull generated by such black hole is responsible for matter accreting towards the centre of the host galaxy. This matter is then released in direction perpendicular to the galactic plane creating jets. These jets produce a non-thermal spectrum that is the result of synchrotron radiation (relativistic electrons travel alongside the magnetic field lines of the jet in helical motion, radiating). This, along with the fact that stars are extremely weak sources at radio wavelengths, allows us to detect jetted AGNs at these wavelengths by basically detecting their jets. We should note at this point, however, that jetted AGNs consist only less than 10% of the total AGN population (more information about AGNs in Padovani (2017),Perlman (2013),Shields (1999)). However, the motivation for searching for alignments is there, as there exist reports of jet alignments in large scale structures (Taylor and

Jagannathan (2016),Contigiani et al. (2017)).

Various mechanisms have been postulated to account for the aforementioned findings. Instrumental biases or contamination from Galactic dust have been largely ruled out (Pelgrims (2019)), as different instruments have produced consistent results, and disparities have emerged between observations at high and low redshifts in relation to polarization vector alignments. A plausible explanation for these alignments revolves around primordial density perturbations. Matter falling into gravitational potential wells undergoes rebound due to radiation pressure, giving rise to oscillations. These oscillations propagate until the epoch of recombination, leaving behind the observed patterns (Kumar Aluri et al. (2023)).

In summary, numerous coherent large scale structures are detected within the cosmic web. In this thesis, I endeavor to investigate whether coherent structures of high statistical significance can be discerned in the sky, employing data from the Very Large Array Sky Survey (VLASS). My approach involves the usage sources taken from the VLASS data, most of which are resolved AGN sources with two or three-component jets from AGNs at kiloparsec scales (we will use the resolved sources only). We aim to verify the regions of significant alignments of parsec-scale jets found by Mandarakas et al. (2021) using our completely independent (and larger) dataset. The thesis is structured as follows: Section 2 details the VLASS data and the quick look images employed in this study; Section 3 delves into the parallel transport of position angle vectors and the S-statistics utilized; Section 4 presents the alignment analysis results; and finally, Section 5 discusses the results and interprets them.

2 Data and data analysis

2.1 The Very Large Array Sky Survey

The Very Large Array Sky Survey (VLASS) is an ambitious project that covers the visible sky observed by the the VLA (Very Large Array) telescope (declination $\geq$ -40 degrees), encompassing a vast expanse of 33885 square degrees. VLASS's observing frequencies span from 2 GHz to 4 GHz, offering spectral and polarimetric data with 2 MHz channel interval, within the radio spectrum. It has an angular resolution of 2.5 arcsec and a remarkable sensitivity of 70 μJy/beam within 1 σ, providing calibrated Stokes polarimetry data for parameters I, Q, and U. The VLASS survey is divided into three epochs, each spanning 32 months, commencing in 2017 and still ongoing. Its primary objectives include addressing four pivotal scientific themes: Hidden explosions and transient events, Faraday tomography of the magnetic sky, Galaxy imaging through time and space, and the detection of radio sources within the Milky Way Galaxy.(Lacy et al. (2020))

To effectively tackle the aforementioned themes, several prerequisites needed to be fulfilled. An angular resolution of at least 3 arcsec (equivalent to 30 kpc at redshifts $\approx$ 1) with an average sensitivity of 120 mJy/beam were deemed essential for identifying sources in cluster fields or those obscured at high redshifts due to dust contamination. This resolution is necessary because most of the objects detected in VLASS are AGN. The resolved sources are mostly kpc jets of AGN since 2.5 arcsecond corresponds to 25 kpc at $z \approx$1. (Lacy et al. (2020))

The observation strategy of VLASS entails recording images of the sky in distinct areas during each configuration cycle of the three epochs (one configuration cycle is an observation of the whole area of the sky that VLA can observe with a duration of 16 months, two configurations make an epoch of observation) conducted by the VLA. In the 2 to 4 GHz range, the VLA's field of view is defined by the primary beam response of its 25-meter diameter antennas. As previously mentioned, a configuration cycle spans 16 months, and each epoch comprises two such cycles. The survey area is divided into tiles, each to be observed for two hours. These tiles are further subdivided into subtiles, defined by their central coordinates. Tiles are organized into 32 tiers based on declination and indexed by Right Ascension (Kimball (2017)).

Once observational data is generated, it is categorized into three classes for processing: Basic Data Products (BDPs), Enhanced Data Products (EDPs) and Services (EDSs), and Commensal Data Products (CDPs). BDPs encompass Raw visibility data (immediately available post-observation), Calibration Data (calibrated through comparison with previous observations of standard calibration sources to eliminate instrumental and other errors), Quick Look images (QL) (expedited production for rapid detection of transient sources, acknowledging potential inaccuracies in coordinate and flux density data) as described in VLASS project Memo13. Single Epoch images (SE) (precisely calibrated images with high data accuracy, including rms noise, spectral indexes, and uncertainties), Single epoch component catalogs (listing the components of sources identified in the single epoch images), Cumulative VLASS images (constructed similarly to single epoch images but incorporating data from all three epochs), and their corresponding Cumulative VLASS component catalog. EDPs and EDSs require external processing, with the Canadian Initiative for Radio Astronomy Data Analysis (CIRADA) (https://cirada.ca/vlasscatalogueql0) project contributing significantly to these aspects. CDPs, on the other hand, rely on external resources and specialized expertise, generated by backend instruments operating in tandem with VLASS. Ideally, it would be great to analyze the cumulative images and detect even single component jets there . However, due to the fact that cumulative images are not ready, and even SE images are available only for 1 percent of the sky, we can not use them. Therefore, we now limit our analysis to catalogues based on the QL images.

2.2 Quick Look images and the CIRADA project

Quick Look images serve as calibrated Stokes I images with a relatively coarse pixel sampling rate of 1 arcsecond per pixel. These data products are primarily designed to facilitate the swift identification of transients, aiming for a one-week interval between tile observations and image completion. To achieve this rapid turnaround, the imaging process employs certain approximations, which presently result in an accuracy limitation of approximately 15% for flux density and a positional accuracy limitation of around 0.3 arcseconds. Consequently, Quick Look images prove most valuable for tasks such as assessing observation quality, detecting transients, and conducting low resolution morphological studies (Lacy et al. (2019)). In this thesis, we will utilize data derived from the Quick Look images of the second epoch, produced by the CIRADA project (Lacy et al. (2022)).

The CIRADA project is a collaborative initiative led by Canadian universities in partnership with NRAO (National Radio Astronomy Observatory) and the Canadian Astronomy Data Center. Its key objectives encompass several crucial areas: creating broadband catalogs containing information about redshifts, morphology, infrared photometry, of detected objects; identification of components within their respective sources; conducting quality assurance for Basic Data Products (BDP) images to identify and rectify common image artifacts that could otherwise be misinterpreted as transient signals; source identification and categorization into catalogs; and the development of a web interface that integrates existing multi-wavelength data, allowing users to filter and identify transients.(Lacy et al. (2020))

The data and catalogs used in this thesis, derived from the CIRADA project. CIRADA has generated catalogs for both epoch 1 and 2 Quick Look images, with plans for a future catalog for the single epoch images. These catalogs consist of three tables: the component table, host ID table, and subtiles information table (for this thesis, only the first two will be utilized from the Quick Look epoch 2 catalog). The component table contains data regarding individual component names, coordinates, sizes, flux, and associated uncertainties. Similarly, the host ID table contains information about the sources that may be comprised of one, two or three components

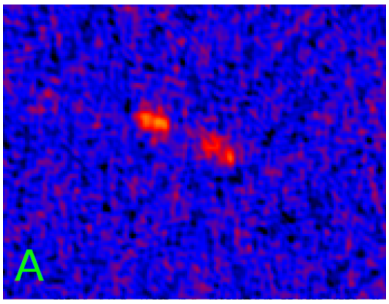

(a) Source with two components

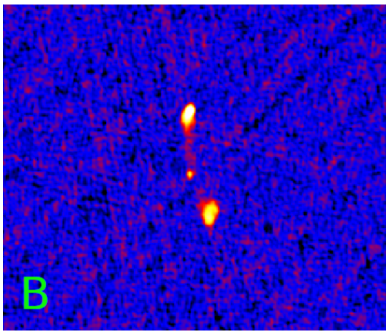

(b) Source with three components

Figure 2.1: Images from sources with two components (right) and three components (left). The components can be seen by the highlighted areas (red-yellow)

from the components table. We are interested in the cases of two and three components which are showcased in 2.1. These two tables can be linked, as the host ID table includes columns that refers to names of components in the corresponding table. To construct this catalog, circular Gaussian fits were applied to the images to detect flux islands above 3σ, with components within these islands identified if they exhibited flux levels 5σ above the noise. The determination of sources employed a likelihood ratio algorithm, akin to methods used in McAlpine et al. (2012). However, since this algorithm was not originally intended for multi-component sources, additional criteria were introduced. For two-component sources, the algorithm compared the position angles of the components of said sources, and if they met certain conditions $|\Delta PA| \leq 30°$ (when comparing the position angle of each individual component), the source was considered less reliable and not recommended for use. Similarly, for three-component sources, a central component was designated (the component closest to the mean RA and DEC of the three components), and if it was not the closest component to the source RA and DEC, it was also marked as not recommended for use(Gordon et al. (2023)).

At this point, it is important to mention some issues with the Quick Look catalogs. Firstly, the flux densities in the Quick Look images are systematically underestimated. To mitigate this, the QL catalog data was compared with a sample from the FIRST catalog, focusing on isolated sources (those without other nearby sources within a 40 arcsecond radius). Secondly, the positional accuracy of VLASS Quick Look (QL) imaging is limited to approximately 1 arcsecond , which improves to 0.3 arcseconds for observations at declinations greater than -20 degrees only. VLASS images from each observing epoch have undergone astrometric offset corrections by the National Radio Astronomy Observatory (NRAO), and these corrections are reflected in the CIRADA epoch-two catalogs. Finally, the host identification process in this catalog is tailored exclusively for radio sources with simple morphologies. It adopts a component isolation philosophy, where no other radio components or sources within 40 arcseconds are found, serving as a rough proxy for the morphological simplicity of a radio source. However, while this approach minimizes the risk of contamination by components within structures smaller than 40 arceseconds, it does not entirely rule out the possibility that the identified source may be part of a larger structure. Such false-positive detections are mitigated by the identification of high-probability host candidates but are not entirely eliminated (see VLASS project memo 3).

In our project, we consider the Position Angles of two and three component AGN sources derived from the coordinates of their components to define their jet directions. Position angle is the angle measured relative to the north celestial pole (NCP), turning positive towards the direction of the right ascension (i,e clockwise), as defined by the International Astronomical Union. In the case of three components, since it is not so trivial, we questioned whether the an angle consisting from the three points of the components in the sky was less than 20 degrees in order for them to be somewhat in a straight line and used the average PA from the PAs between the component that was in the top of the angle and the other two. Then, we use these PAs to perform statistical analysis and tried to find alignments in the 2D plane of the sky[1]. Originally, the component table contains 2995271 components while the host table has 694973 sources. In order to manipulate these large data sample (1.1 GB for the component catalog and 100 MB for the host ID catalog) we had to create a relational database in MariaDB engine. Then, using SQL language and python scripts we matched the sources with their components while also excluding the single component sources from our data sample. We made catalogs containing the sources with their components and their respective coordinates and used the data

[1]At this point it should be mentioned that what we use later should be called "an AGN structural axis", but for most of the source in the sample it is the jet direction and we will call it this way along the thesis.

of 31507 sources with two components and those of 1060 sources with three components.

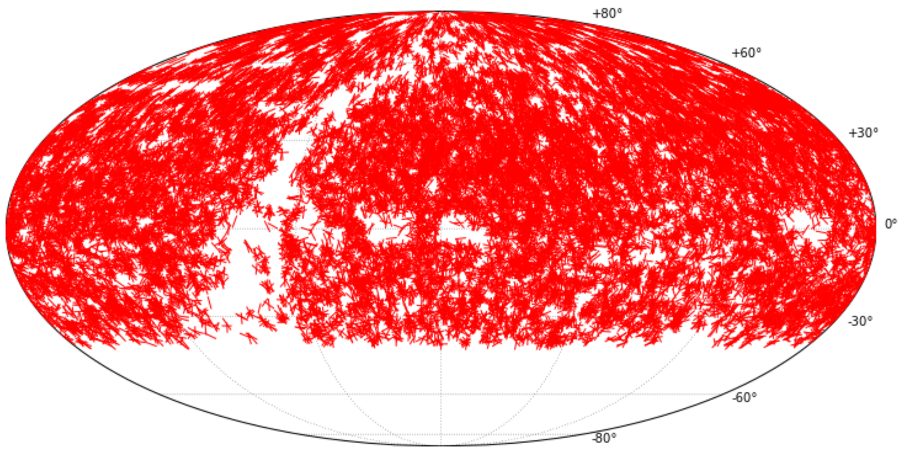

Figure 2.2: Distribution of determined structural axes of radio sources in VLASS QL data. The plot is in Mollweide projection and is in equatorial reference frame.

3
Alignments tests

3.1 Parallel transport

In this thesis, as mentioned before, we use the Position Angles of sources. The jet direction we identified in the previous section can be considered as unit vector tangent to the celestial sphere to measure the angle between that and the celestial meridian. For two such vectors lying on different points in the sky, their position angles can not be compared since they are lying on different reference systems. To solve this problem we use the the notion of parallel transport to have the two angles be in the same reference frame.

We use the method described in Contigiani et al. (2017) to perform the parallel transport. We parameterize a vector lying tangent to the sphere (in this work we have 2D information and therefore we consider all vectors tangent to the celestial sphere) with coordinates $\hat{e_r}, \hat{e_\theta}, \hat{e_\phi}$ (which are three unit vectors towards the center, north and east of the sphere respectively) defining an orthonormal coordinate system to the sphere. The unit vector representing the jet can then be defined as

$$\hat{\nu} = \cos\alpha \ \hat{e_\theta} + \sin\alpha \ \hat{e_\phi} \tag{3.1}$$

where the α is the position angle of the jet. One can see immediately that position angle is dependent on the choice of the orthonormal system and therefore on the location the jet has on the celestial sphere. However, we can now define a coordinate-invariant inner product for two vectors lying on different points when translating the vectors along the arc of the great circle that connects them. Consider two vectors lying on points P_1 and P_2 with spherical coordinates r, θ, ϕ. The vector perpendicular to the great circle connecting the two would be

$$\hat{e_s} = \frac{\hat{e_{r_1}} \times \hat{e_{r_2}}}{|\hat{e_{r_1}} \times \hat{e_{r_2}}|} \tag{3.2}$$

and the vectors tangent to the great circle connecting P_1 to P_2 and P_2 to P_1 respectively would be

$$\hat{e_{t_1}} = \hat{e_s} \times \hat{e_{r_1}} \tag{3.3}$$

and

$$\hat{e_{t_2}} = \hat{e_s} \times \hat{e_{r_2}} \tag{3.4}$$

respectively. We call θ the angle between $\hat{\nu_1}$ and $\hat{e_{t_1}}$. This angle remains invariant as $\hat{\nu_1}$ is being transported on the great circle and thus the translated position angle is

$$\alpha_1{}' = \alpha_1 + \beta_2 - \beta_1, \tag{3.5}$$

where β_1 the angle between $\hat{e_{\theta_1}}$ and $\hat{e_{t_1}}$ and β_2 the angle between $\hat{e_{\theta_2}}$ and $\hat{e_{t_2}}$. The dot product between the two is

$$(\alpha_1, \alpha_2) = \cos\left[2(\alpha_1 - \alpha_2 + \beta_2 - \beta_1)\right], \tag{3.6}$$

since $\hat{v_1}$ and $\hat{v_2}$ are unit vectors. The factor 2 comes from the fact that the PAs in our data range from $-\pi/2$ to $\pi/2$.

3.2 Statistical analysis

The calculations performed here are done in the same manner as in Mandarakas et al. (2021). In this study to search for potential directional alignments among jets in specific sky regions, we used the S-test. Introduced by Hutsemekers (1998b), the S-test was initially designed to statistically quantify alignments of polarization vectors across the celestial sphere. This test relies on assessing the dispersion of position angles within a group of nearby sources drawn from the main sample. Jain et al. (2004) later devised a computationally efficient variant of the test, which was adopted for this study.

For a designated region of interest, denoted as “i,” encompassing n celestial sources, we aimed to identify a central position angle, ξ, that best characterizes the average position angle of these sources. To accomplish this,

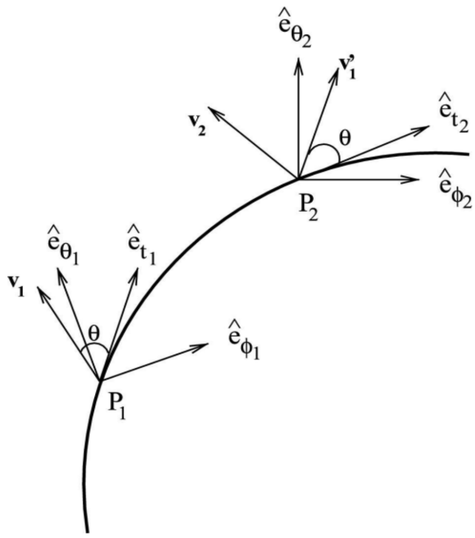

Figure 3.1: Visualisation of parallel transport from P_1 to P_1 as described in Contigiani et al. (2017). The $\hat{\nu}$ vectors stand for Jet PA vectors and $\hat{v_1'}$ vector is the Jet PA vector from the jet in position P_1 when transported to position P_2, $\hat{e_t}$ vectors are the vectors tangents to the line of the great circle and $\hat{e_\theta}$ and $\hat{e_\phi}$ are the unit vectors towards the north and east of the sphere for the two positions respectively.

we examined their position angle unit vectors, $\xi_1, \xi_2, \ldots, \xi_n$, and formulated the following quantity:

$$d_{i,n}(\boldsymbol{\xi}) = \frac{1}{n}\sum_{i=1}^{n}(\xi, \xi'_k). \tag{3.7}$$

Here, ξ'_k represents the new position angle unit vector for the kth source, parallel-transported to the region's center, and $\boldsymbol{\xi}$ denotes the unit vector of ξ. The parameter $d_{i,n}(\boldsymbol{\xi})$ serves as an indicator of how closely the source jets align with $\boldsymbol{\xi}$. The angle that corresponds to the mean direction of the jet position angles is the one that maximizes this expression. This formulation is encapsulated in the following expression:

$$D_{i,n} = d_{i,n}|_{max} = \frac{1}{n}[(\sum_{i=1}^{n} cos2\xi'_k)^2 + (\sum_{i=1}^{n} sin2\xi'_k)^2]^{1/2} \tag{3.8}$$

Here, higher values of $D_{i,n}$ imply a stronger alignment, with $D_{i,n} = 1$ indicating perfect alignment and $D_{i,n} = 0$ meaning complete uniformity. To quantify the alignment's significance, we defined the significance level (SL) in a manner akin to Contigiani et al. (2017)

$$SL = 1 - \Phi(\frac{D_{i,n} - \langle D_{i,n}\rangle_{\mathrm{MC}}}{\langle \sigma_{i,n}\rangle_{\mathrm{MC}}}) \tag{3.9}$$

In this equation, Φ represents the normal cumulative distribution function. $\langle D_{i,n}\rangle_{\mathrm{MC}}$ represents the average $D_{i,n}$ value for the ith region, computed through Monte Carlo (MC) simulations assuming random PA distributions across the sky. Similarly, $\langle \sigma_{i,n}\rangle_{\mathrm{MC}}$ is the standard deviation of the simulated $D_{i,n}$ values for that region. To obtain SL values, MC simulations were conducted, where new PA values were assigned to all sources in our sample drawn from a uniform distribution. Then $D_{i,n}$ was calculated for the region using these random PA assignments. After 10,000 repetitions, we derived the average and standard deviation to compute SL.

For interpretive purposes, confidence levels of multiples of σ correspond to specific values of $\log(SL)$, where $\log(SL) < -6.24$ signifies confidence exceeding 5σ, in order to know how often does the presented alignment appear randomly. This allows us to assess the degree of alignment in the jet position angles within the selected sky regions.

4
Search for alignments in VLASS QL data

The principal objective of this statistical analysis is to investigate whether significant alignments exist within the regions previously identified in Mandarakas et al. (2021). The aim is to test whether the significant alignments of parsec scale AGN jets also exist in an independently observed sample of kiloparsec-scale jets. Upon conducting the analysis, iwe found that there are no alignments present in the specific areas pinpointed by Mandarakas et al. (2021) in VLASS data. However, noteworthy alignments are discovered within our data sample, albeit in different sections of the celestial sphere.

4.1 Search for alignments in areas of possibly coherent structures as defined from parsec scale radio jets

As it was discussed before,Mandarakas et al. (2021) found 4 regions where parsec-scale jets show significant ($>5\sigma$) alighnment. Using our indepenent dataset we aim to check whether these alignments are spurious or real. For that reason, we perform an S-test on the on the regions previously defined in Mandarakas et al. (2021) and present our results bellow.

The distribution of found kiloparsec-scale jets directions as well as parscec-scale jets directions from Mandarakas et al. (2021) in the regions with previously found significant alignments are shown in Figs. 4.1 and 4.2. These

ID	$\log SL$	RA (deg)	DEC (deg)	radius (deg)	SL (σ)
QJAR1	-0.806	36.18	25.95	14.82	1.418
QJAR2	-0.739	168.75	47.54	18.11	1.333
QJAR3	-0.503	180.15	23.56	16.07	1.007
QJAR4	-0.591	201.83	50.97	18.27	1.134

Table 4.1: Results of using the VLASS data in search of alignments. We define the coordinates of each area and its radius as well as the significance of the alignments. The regions are the QJAR areas found in Mandarakas et al. (2021) and the parameters are from the same paper with the exception of the values about SL which are calculated using our data in the exact same areas.

figures illustrate these areas, depicting the jets of our data sample within the QJAR (Quasar Jet Alignment Regions) areas, and Fig. 4.2 shows distributions of Jet PAs (Position Angles) and telescope Beam PAs in the same regions . The sample of parsec-scale jets from Mandarakas et al. (2021) demonstrates a preferred direction (their SL values in σ are higher than 5), whereas the VLASS sample produces no such patterns. In Mandarakas et al. (2021), the search for alignments was also redshift-dependent, which means it was a 3D analysis, whereas our study was limited to a 2D approach. Consequently, our sample potentially encompasses a significantly greater number of sources than those considered in Mandarakas et al. (2021). This difference in the analysis can potentially explain the difference in the results. It could be that the alignments are indeed present in a narrow range of redshifts. Then considering jets at all possible redshifts, we contaminate the aligned sample with jets of random directions.

We present a table 4.1 summarizing our search for alignments and provide a comparative analysis of our SL (Significance Level) values with those found in the table from Mandarakas et al. (2021).

At this point is important to add that parsec and kiloparsec-scale jets can be misaligned (McKinney et al. (2013)). This happens because of jet bending. This is probably a result of the interaction of jets with the ambient medium surrounding them (Vazza et al. (2021)). This leads to a change of the PA of the jet being projected on the sky. As such it is important that we compare common sources in our sample with those in Mandarakas et al.

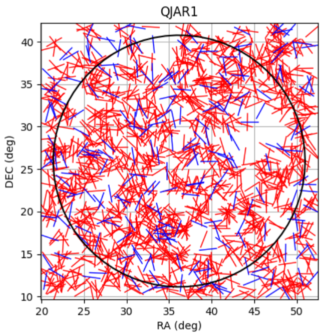

(a) QJAR1

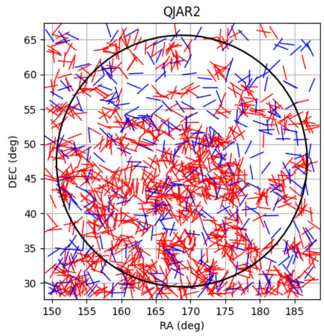

(b) QJAR2

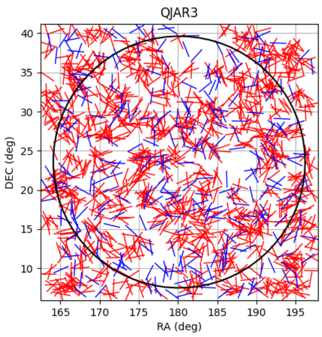

(c) QJAR3

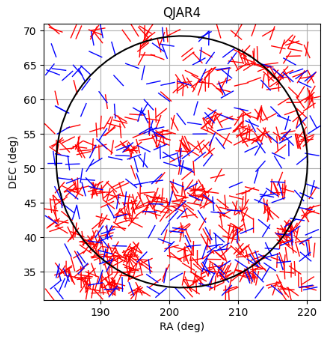

(d) QJAR4

Figure 4.1: 2D plots of the areas presented in Mandarakas et al. (2021) named QJARs. With blue the jets from Mandarakas et al. (2021)'s research are shown, and with red our data for the PAs of the jets. By close examination one can see that the blue jets have some level of alignment while the VLASS data don't.

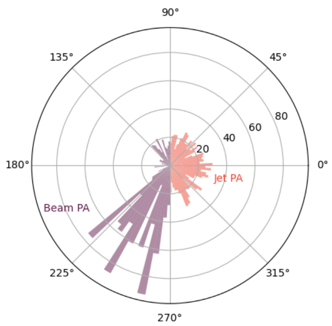

(a) QJAR1

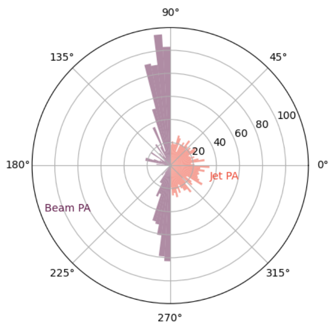

(b) QJAR2

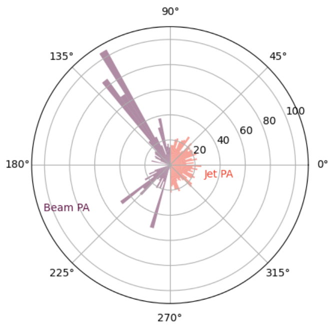

(c) QJAR3

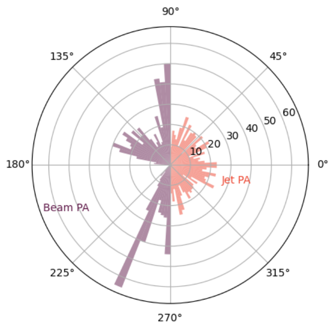

(d) QJAR4

Figure 4.2: Bipolar plots of Jet PAs and Beam PAs using VLASS data in QJARs. Both Jet PAs and Beam PAs range from -90 to 90 degrees (All Beam PAs have been increased by 180 degrees so that they can be plotted). These plots include only sources in the QJARs for which we can have Beam PA information. No significant preferences are appearing in the values of PAs in comparison to the rest of the plotted sample.

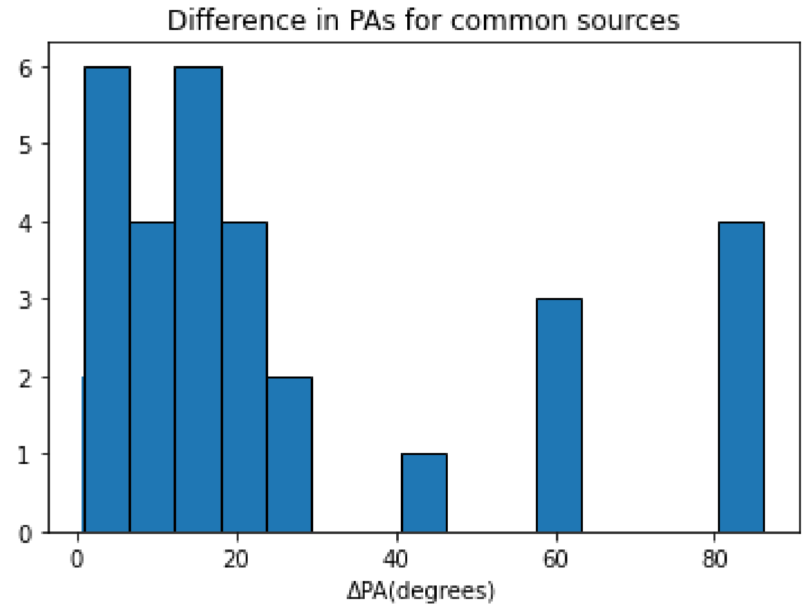

Figure 4.3: Histograms of $\Delta|PA_{\mathrm{Kpc}} - PA_{\mathrm{pc}}|$. There is a clear peak at $PA \approx 0$. The maximum separation of those sources is 15 arcseconds

(2021). We perform this comparison by identifying sources with separations of less than 5, 10, 15, and 20 arcseconds, employing a straightforward methodology. After identifying and pairing these sources, we compare their Position Angles using the formula $\Delta|PA_{\mathrm{Kpc}} - PA_{\mathrm{pc}}|$. After our analysis we generate histograms plotting the number of pairs versus ΔPA. We present one of those histograms for separations less than 15 degrees (Fig. 4.3). A clear tendency for most of the sources to have a ΔPA close to 0 is shown. Thus we conclude that the information about internal jet direction is not lost at kiloparsec scale and thus we can correlate our sample with the one from Mandarakas et al. (2021)

4.2 Search for regions with significant alignments of AGN jets in the VLASS data

Using the newly acquired sample of kiloparsec-scale jets from VLASS we performed a search for alignments in the whole sky area covered by our data with the goal of finding Areas of jet alignments (from this point on, we will refer to them as AAJA, AGN Areas of Jet Alignments, in order to distinguish from QJARs by Mandarakas et al. (2021)). We searched the whole available area using circles with radii values of 5, 6, 7, 11 and 13 degrees with the centers of the circles ranging between -50 to 90 degrees in declination and 0 to 360 degrees in right ascension. For each value of declination, we placed grids of such circles in ascending order of RA with separation between the centers of the circles being equal to their radii and after each loop was finished, we increased the value of declination by the radius value. We repeated the same process for each circle. We found 8 areas in which the significance level exceeded 5 σ . From these areas we picked only the most significant of them since some of them were overlapping for different values of radii. We present the values of significance level in the following table as well as figures of these four locations showing the jets (tab. 4.2, Fig. 4.4), circular histograms of Jet PAs and beam PAs and finally a whole map of the sky (FIg. 4.5) showcasing these regions.

ID	$\log SL$	RA (deg)	DEC (deg)	radius (deg)	avgPA (deg)	SL (σ)
AAJA1	-6.25	182	-37	13	-86.53	5.005
AAJA2	-11.25	221	-11	13	-82.47	6.888
AAJA3	-8.03	338	-11	13	-74.96	5.742
AAJA4	-8.97	143	-6	11	-54.43	6.099

Table 4.2: Results of using the VLASS data in search of alignments. We present the coordinates of each area and its radius as well as the significance of the alignments.

Despite the formally found high significance of the detection of alignment, there is the possibility that this alignments are spurious and caused by systematic biases and uncertainties. As described in section 2.2, the use of quick look images induces systematics and false detections of sources are possible, especially for detections with declination below -20 degrees and the areas AAJA1, AAJA2 and AAJA3 include such detections. In 3 out of 4 regions the preferred Jet PA direction is on average perpendicular to the Beam PA preferred direction. This means that the detected Jet PA

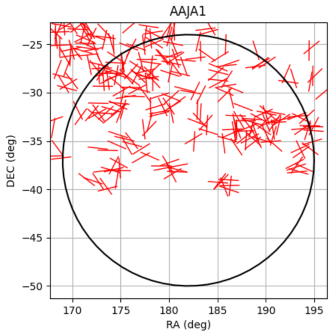

(a) AAJA1

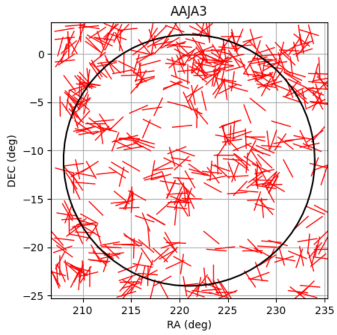

(b) AAJA2

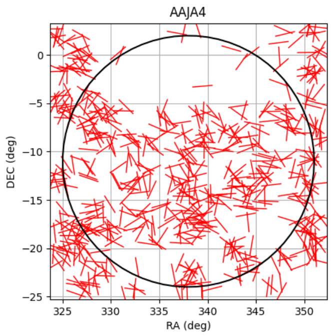

(c) AAJA3

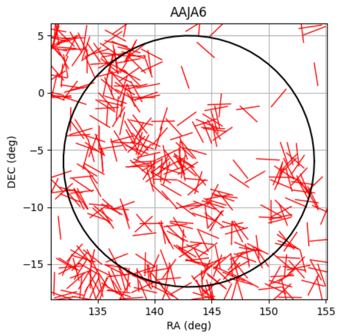

(d) AAJA4

Figure 4.4: 2D plots of the areas from our data. With red our data for the PAs of the jets. By close examination one can see that the jets have some level of alignment.

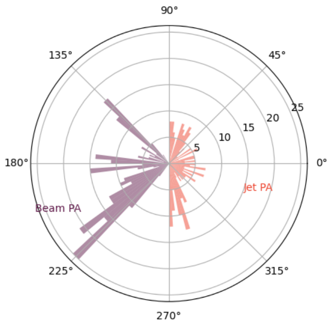

(a) AAJA1

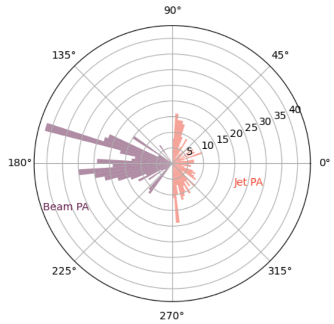

(b) AAJA2

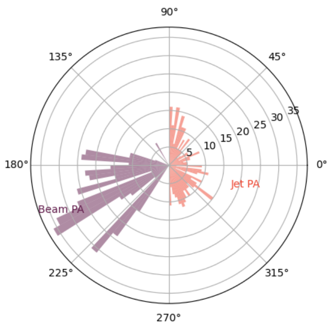

(c) AAJA3

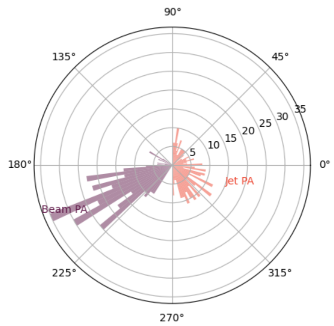

(d) AAJA4

Figure 4.5: Polar plots of Jet PAs and Beam PAs. Both Jet PAs and Beam PAs range from -90 to 90 degrees (All Beam PAs have been shifted by 180 degrees so that they can be plotted). These plots include only sources in the AAJAs for which we can have the Beam PA information. Significant deviation from the uniform distribution is obvious for both Jet and Beam PA in all four histograms. In AAJA1-AAJA3 the preferred Jet PA is in the 90 - 270 degrees direction, while in AAJA4 the Jet PA tends to be pointing along the 135 - 315 degrees plane.

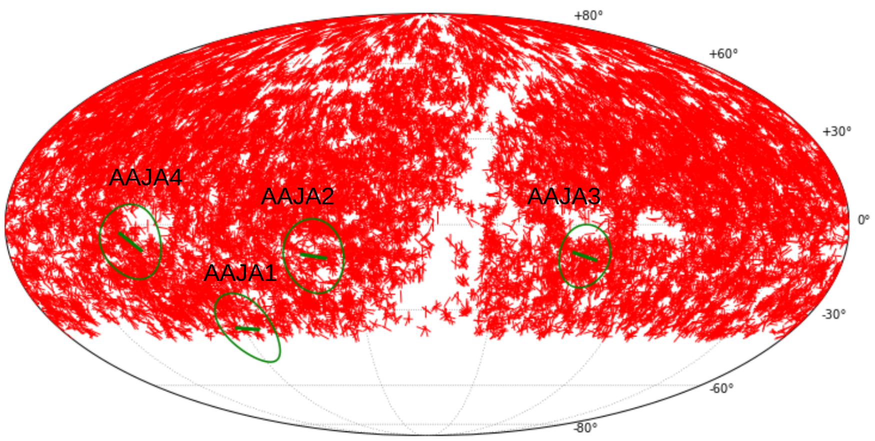

Figure 4.6: Distribution of determined jet PAS of radio sources in VLASS QL data. The plot is in Mollweide projection and is in equatorial reference frame, this time AAJAs are included representing the regions of high significant alignment. From left to right we see the areas AAJA4, AAJA1, AAJA2 and AAJA3

tends to be along the plane where VLA has better resolution. In AAJA4 we see a similar effect: the peak in the distribution of Jet PA is perpendicular to the prominent peak in the beam PA. That is why, it is very likely that the detected alignments are a systematic effect. Another issue, this time concerning AAJA1 specifically is the fact that we don't have data for DEC <-40 degrees, meaning that this particular area may not have significant alignments if data for the whole area were available as shown in figures 4.6 and 4.5d. At this point it should be mentioned, however, that we do not have beam PA information for all the jets because the information about jet PA came from the beam PA of their respective components and some of them had completely different values for the beam PA while belonging to the same source. Thus the results for beam PA could be misleading. Further investigation of these four areas is needed where we will include redshift information, however we won't include it in this work.

5
Summary and Conclusions

The universe appears to contain coherent structures in which the jets of AGNs appear to have preferred directions. Motivated by this Mandarakas et al. (2021) searched and found such coherent structures. In a similar fashion, we tried to use data of 2 or 3 component AGN sources, detected in radio wavelengths (of 2 to 4 GHz) by VLASS. We used the epoch 2 catalog of Quick Look images made by the CIRADA project to find the coordinates of said sources and their components. After processing the data in these catalogs we found Jet PAs for all sources and made a 2D search for alignments in the areas previously detected by Mandarakas et al. (2021) using our data. After that we also performed independent all-sky search of alignment using this new data sample.

Our results show no alignments in the areas previously detected by Mandarakas et al. (2021) (QJARs). However, we detect four different regions where significant alignments are present in our data (AJAAs). The reason for not finding significant alignments as in Mandarakas et al. (2021) in their regions is probably because we made a 2D research of the sky whereas they did a 3D. For our data, without exceptions, the areas of alignment we present are quite possibly produced by systematic biases either generated by inaccuracies that the low quality of the quick look images induced or by lack of data in the sample (e.g. AAJA1).

The 2D research, although useful in regards to pointing out areas for further research, is not trustworthy for the detection of cosmological structures (for instance filaments) since it lacks redshift information. Thus, even in our data, even though we do have areas of alignment with significance level greater than 5 σ, the likelihood of this level being produced by other sources in the same areas of the sky sphere but by sources in different redshifts can not be ignored. For that reason, our future plans include a study with the same data sample, with the difference that this time we will include redshift information from The Million Quasars (Milliquas) Catalogue (Flesch (2023)).

Finally, we need to address the possibility of AAJAs being produced purely by randomness. This is especially an issue for areas with SL close to 5 sigma. To test this hypothesis you we must run an MC simulation, where we generate hundreds of millions of mock samples similar to he sample from the VLASS data and repeat the whole procedure of search of alignments. For this, we will require a powerful computational cluster of computers and so we will test this in the future.

A good indicator of this is the fact that PAs for sources with declinations bellow $-20°$ don't have a uniform distribution. We performed the KS uniformity test for the jet PAs of such sources and found p-value = 0.000017. As we can see in Fig. 5.1 these PAs form a peak around the value of 90 degrees. This happens probably because of the angular resolution of sources in these declinations as mentioned in section 2.2.

To further showcase this issue we will perform the following thought experiment. Suppose that our sample has a completely random collection of sources with a distribution of PAs shown in Fig. 5.1. To search for alignments in our sample we performed a scan in that area of the sky using tangent circles with radii of 11 and 13 degrees, performing 110 and 88 trials for each circle respectively. The average number of sources contained in each circle would be

$$n_{sources\ in\ circle} = \frac{Area\ of\ circle}{Area\ of\ the\ observed\ sky} N_{total\ number\ of\ sources}. \tag{5.1}$$

The question we pose is: what is the probability of finding 50%[1] or more of the sources detected in any of those circles to be in range of 54 to 117 degrees[2] (of the total 180 degree range) with the rest being randomly distributed in such sample (we consider such area to have alignment)? This question is the same as: what is the probability of finding at least one significant alignment in a circle of this sample? The answer for each circle would be given by a hypergeometric distribution (since we pick n sources from a greater sample

[1]percentage of sources with jet PAs lying in the range of 54 to 117 degrees that yield significant alignments

[2]we pick that range of PAs because of the peak shown in Fig.5.1

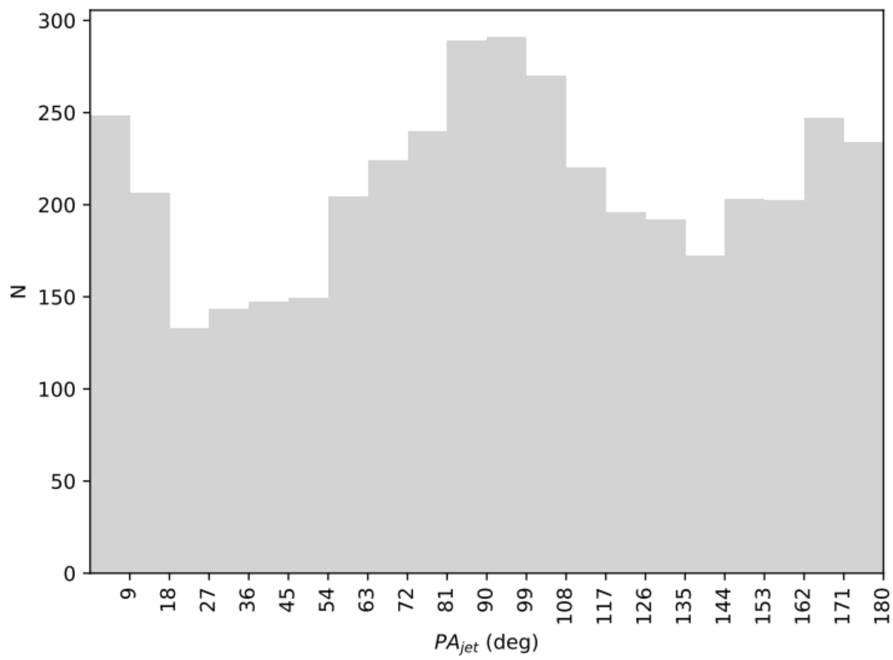

Figure 5.1: Histogram of jet PAs with declination$> -20°$. This distribution of PAs diverges from uniformity and has a p-value=0.000017 as derived from the KS uniformity test.

of sources in which approximately 46%, which is the percentage of sources lying in the desired PA range, of them have the desired quality and we need 50% of the picked sample to have the desired quality). Of course, since the number of total sources is far greater than the ones in the circle the probability for finding at least one alignment in one circle for one trial would be given by a normal distribution Φ as:

$$P = \int_{n}^{\infty} \Phi(x)dx. \tag{5.2}$$

The total probability for all trials is:

$$P_{total} = P_{r=11}^{N_{tr,r=11}} P_{r=13}^{N_{tr,r=13}}, \tag{5.3}$$

where N_{tr} is the total number of trials for each circle. We find this probability to be $\frac{1}{2591546380}$ which is less than the probability of finding an aligned area with significance level of more than 5 σ ($\frac{1}{1744278}$). So with that rough approximation in mind, we conclude that all the AAJAs we found are a result of systematics.

Bibliography

Tracey Friday. Correlations between multiple tracers of the cosmic web. *arXiv e-prints*, art. arXiv:2009.01637, September 2020. doi: 10.48550/arXiv.2009.01637. 1, 2

B. V. Komberg, A. V. Kravtsov, and V. N. Lukash. The search for and investigation of large quasar groups. *Monthly Notices of the Royal Astronomical Society*, 282(3):713–722, 10 1996. ISSN 0035-8711. doi: 10.1093/mnras/282.3.713. URL `https://doi.org/10.1093/mnras/282.3.713`. 1

Roger G. Clowes, Kathryn A. Harris, Srinivasan Raghunathan, Luis E. Campusano, Ilona K. SÃ¶chting, and Matthew J. Graham. A structure in the early universe at z $\sim$ 1.3 that exceeds the homogeneity scale of the r-w concordance cosmology. *Monthly Notices of the Royal Astronomical Society*, 429(4):2910–2916, jan 2013. doi: 10.1093/mnras/sts497. 1

H. Lietzen, E. Tempel, L. J. LiivamÃ¤gi, A. Montero-Dorta, M. Einasto, A. Streblyanska, C. Maraston, J. A. RubinÃ$\mu - Mart$Ã-$n, andE.\ Saar.$2016.1

Pavan Kumar Aluri, Paolo Cea, Pravabati Chingangbam, Ming-Chung Chu, Roger G. Clowes, Damien Hutsemékers, Joby P. Kochappan, Alexia M. Lopez, Lang Liu, Niels C. M. Martens, C. J. A. P. Martins, Konstantinos Migkas, Eoin Ó Colgáin, Pratyush Pranav, Lior Shamir, Ashok K. Singal, M. M. Sheikh-Jabbari, Jenny Wagner, Shao-Jiang Wang, David L. Wiltshire, Shek Yeung, Lu Yin, and Wen Zhao. Is the observable Universe consistent with the cosmological principle? *Classical and Quantum Gravity*, 40(9):094001, May 2023. doi: 10.1088/1361-6382/acbefc. 1, 2, 3

D. Blinov, C. Casadio, N. Mandarakas, and E. Angelakis. Global alignments of parsec-scale AGN radio jets and their polarization planes. *A&A*, 635:A102, March 2020. doi: 10.1051/0004-6361/202037444. 1

D Hutsemekers. Evidence for very large-scale coherent orientations of quasar polarization vectors, 1998a. URL `http://cdsweb.u-strasbg.fr/Abstract.html`. 1

S. A. Joshi, R. A. Battye, I. W.A. Browne, N. Jackson, T. W.B. Muxlow, and P. N. Wilkinson. A survey of polarization in the jvas/class flat-spectrum radio source surveys - ii. a search for aligned radio polarizations. *Monthly Notices of the Royal Astronomical Society*, 380:162–174, 2007. ISSN 13652966. doi: 10.1111/j.1365-2966.2007.12028.x. 2

Prabhakar Tiwari and Pankaj Jain. Polarization alignment in jvas/class flat spectrum radio surveys. 1 2012. doi: 10.1142/S0218271813500892. URL `http://arxiv.org/abs/1201.5180http://dx.doi.org/10.1142/S0218271813500892`. 2

Prabhakar Tiwari and Pankaj Jain. Evidence of isotropy on large distance scales from polarizations of radio sources. *Astronomy and Astrophysics*, 622, 2 2019. ISSN 14320746. doi: 10.1051/0004-6361/201834192. 2

William d'Assignies D., Nora Elisa Chisari, Nico Hamaus, and Sukhdeep Singh. Intrinsic alignments of galaxies around cosmic voids. 2021. 2

Christos Georgiou, Harry Johnston, Henk Hoekstra, Massimo Viola, Konrad Kuijken, Benjamin Joachimi, Nora Elisa Chisari, Daniel J. Farrow, Hendrik Hildebrandt, Benne W. Holwerda, and Arun Kannawadi. The dependence of intrinsic alignment of galaxies on wavelength using kids and gama. *Astronomy and Astrophysics*, 622, 2 2019. ISSN 14320746. doi: 10.1051/0004-6361/201834219. 2

Giovanni Camelio and Marco Lombardi. On the origin of intrinsic alignment in cosmic shear measurements: An analytic argument. *Astronomy and Astrophysics*, 575:1–11, 3 2015. ISSN 14320746. doi: 10.1051/0004-6361/201425016. 2

Paolo Padovani. Active galactic nuclei at all wavelengths and from all angles, 11 2017. ISSN 2296987X. 2

Eric S. Perlman. *Active Galactic Nuclei*, pages 305–386. Springer Netherlands, Dordrecht, 2013. ISBN 978-94-007-5609-0. doi: 10.1007/978-94-007-5609-0_7. URL `https://doi.org/10.1007/978-94-007-5609-0_7`. 2

Gregory A. Shields. A brief history of active galactic nuclei. *Publications of the Astronomical Society of the Pacific*, 111(760):661, jun 1999. doi: 10.1086/316378. URL `https://dx.doi.org/10.1086/316378`. 2

A. R. Taylor and P. Jagannathan. Alignments of radio galaxies in deep radio imaging of ELAIS N1. *Monthly Notices of the Royal Astronomical Society: Letters*, 459(1):L36–L40, 03 2016. ISSN 1745-3925. doi: 10.1093/mnrasl/slw038. URL `https://doi.org/10.1093/mnrasl/slw038`. 2

O. Contigiani, F. de Gasperin, G. K. Miley, L. Rudnick, H. Andernach, J. K. Banfield, A. D. KapiÅska, S. S. Shabala, and O. I. Wong. Radio galaxy zoo: Cosmological alignment of radio sources. *Monthly Notices of the Royal Astronomical Society*, 472:636–646, 2017. ISSN 13652966. doi: 10.1093/MNRAS/STX1977. 3, 11, 13, 14

V. Pelgrims. Cosmological-scale coherent orientations of quasar optical polarization vectors in the planck era: Investigating the galactic dust contamination scenario. *Astronomy and Astrophysics*, 622, 2 2019. ISSN 14320746. doi: 10.1051/0004-6361/201731294. 3

N. Mandarakas, D. Blinov, C. Casadio, V. Pelgrims, S. Kiehlmann, V. Pavlidou, and K. Tassis. Local alignments of parsec-scale AGN radiojets. *A&A*, 653:A123, September 2021. doi: 10.1051/0004-6361/202140764. 3, 12, 15, 16, 17, 19, 20, 25

M. Lacy, S. A. Baum, C. J. Chandler, S. Chatterjee, T. E. Clarke, S. Deustua, J. English, J. Farnes, B. M. Gaensler, N. Gugliucci, G. Hallinan, B. R. Kent, A. Kimball, C. J. Law, T. J.W. Lazio, J. Marvil, S. A. Mao, D. Medlin, K. Mooley, E. J. Murphy, S. Myers, R. Osten, G. T. Richards, E. Rosolowsky, L. Rudnick, F. Schinzel, G. R. Sivakoff, L. O. Sjouwerman, R. Taylor, R. L. White, J. Wrobel, H. Andernach, A. J. Beasley, E. Berger, S. Bhatnager, M. Birkinshaw, G. C. Bower, W. N. Brandt, S. Brown, S. Burke-Spolaor, B. J. Butler, J. Comerford, P. B. Demorest, H. Fu, S. Giacintucci, K. Golap, T. GÃ¼th, C. A. Hales, R. Hiriart, J. Hodge, A. Horesh, IveziÄ, M. J. Jarvis, A. Kamble, N. Kassim, X. Liu, L. Loinard, D. K. Lyons, J. Masters, M. Mezcua, G. A. Moellenbrock, T. Mroczkowski, K. Nyland, C. P. Oâdea, S. P. Oâsullivan, W. M. Peters, K. Radford, U. Rao, J. Robnett, J. Salcido, Y. Shen, A. Sobotka, S. Witz, M. Vaccari, R. J. van Weeren, A. Vargas, P. K.G. Williams, and I. Yoon. The karl g. jansky very large array sky survey (vlass). science case and survey design. *Publications of the Astronomical Society of the Pacific*, 132, 3 2020. ISSN 00046280. doi: 10.1088/1538-3873/ab63eb. 5, 7

Amy E Kimball. Vlass project memo 7 vlass tiling and sky coverage, 2017. URL `http://goo.gl/znDX0i`. 6

Mark Lacy, Claire Chandler, Amy Kimball, Steve Myers, Kristina Nyland, Stephan Witz, and Vlass Team. The vla sky survey-operations, data processing and archiving, 2019. 7

M Lacy, S T Myers, C Chandler, A D Kapinska, B Kent, A Kimball, J Marvil, J Masters, D Medlin, K Radford, F Schinzel, L Sjouwerman, A Sobotka, and A Vargas. Vlass project memo 13: Pilot and quick look data release (v2), 2022. URL `https://science.nrao.edu/science/surveys/vlass/`. 7

Kim McAlpine, Dan J. B. Smith, Matthew J. Jarvis, David G. Bonfield, and Simone Fleuren. The likelihood ratio as a tool for radio continuum surveys with ska precursor telescopes. 2 2012. doi: 10.1111/j.1365-2966.2012.20715.x. URL `http://arxiv.org/abs/1202.1958http://dx.doi.org/10.1111/j.1365-2966.2012.20715.x`. 8

Yjan Gordon, Adrian Vantyghem, Biny Sebastian, Lawrence Rudnick, Heinz Andernach, and Michelle Boyce. Cirada: Vlass catalog user guide, 2023. 8

D Hutsemekers. Evidence for very large-scale coherent orientations of quasar polarization vectors, 1998b. URL `http://cdsweb.u-strasbg.fr/Abstract.html`. 12

Pankaj Jain, Gaurav Narain, and S. Sarala. Large-scale alignment of optical polarizations from distant qsos using coordinate-invariant statistics. *Monthly Notices of the Royal Astronomical Society*, 347:394–402, 1 2004. ISSN 00358711. doi: 10.1111/j.1365-2966.2004.07169.x. 12

Jonathan C. McKinney, Alexander Tchekhovskoy, and Roger D. Blandford. Alignment of magnetized accretion disks and relativistic jets with spinning black holes. *Science*, 339(6115):49–52, January 2013. ISSN 0036-8075. doi: 10.1126/science.1230811. 16

F. Vazza, D. Wittor, G. Brunetti, and M. BrÃ¼ggen. Simulating the transport of relativistic electrons and magnetic fields injected by radio galaxies in the intracluster medium. 2 2021. doi: 10.1051/0004-6361/202140513. URL http://arxiv.org/abs/2102.04193http://dx.doi.org/10.1051/0004-6361/202140513. 16

Eric Wim Flesch. The million quasars (milliquas) catalogue, v8. 8 2023. URL http://arxiv.org/abs/2308.01505. 26